Promoting effect of Pt addition to $Ni/CeO_2/Al_2O_3$ catalyst for steam gasification of biomass

Jin Nishikawa, Tomohisa Miyazawa, Kazuya Nakamura, Mohammad Asadullah, Kimio Kunimori, Keiichi Tomishige*

Institute of Material Sciences, University of Tsukuba, 1-1-1, Tennodai, Tsukuba, Ibaraki 305-8573, Japan

Corresponding author: Keiichi Tomishige

Tel + Fax: +81-298-53-5030, E-mail: tomi@tulip.sannet.ne.jp

Abstract

The modification of $Ni/CeO_2/Al_2O_3$ with Pt can make the activation by H_2 reduction unnecessary, and this indicates that the $Pt/Ni/CeO_2/Al_2O_3$ catalyst can be activated automatically by the compounds contained in tar. This can be explained by the enhancement of the Ni reducibility by the addition of Pt. The results of the temperature programmed reduction with H_2 also support this enhancement. Furthermore, the addition of 0.1% Pt to $Ni/CeO_2/Al_2O_3$(4wt% Ni, 30wt% CeO_2) enhanced the performance in the steam gasification of biomass, compared to Ni/Al_2O_3 and $Ni/CeO_2/Al_2O_3$ in terms of low tar yield and high gas yield. This can be related to the Pt-Ni alloy formation indicated by the extended X-ray absorption fine structure analysis.

Keywords

Steam gasification, Steam reforming, Ni, Pt, Tar, Coke, Biomass, Activation, Reduction, Regeneration

Introduction

Conversion of biomasses to hydrogen and synthesis gas becomes more and more important in terms of the utilization of renewable sources [1]. In the non-catalytic gasification with air which is one of the conventional syngas and hydrogen production methods from biomass, high reaction temperature is required to the tar removal [2]. The application of metal catalysts in the biomass gasification system is an effective approach to reduce the tar content [2-4]. In most cases, commercially available, steam reforming Ni catalysts have been applied, and the problem of catalyst deactivation due to coke deposition has been pointed out [2-4]. Recently, our group has reported the gasification of cellulose [5-7] and biomass [8-13] with air using $Rh/CeO_2/SiO_2$. It is found that $Rh/CeO_2/SiO_2$ was much more effective catalyst for the gasification of biomass with air than conventional steam reforming Ni catalyst and dolomite. In particular, it also showed high resistance to coke deposition and high stability [5-13].

From the practical viewpoint, the gasification of biomass with air gives the gaseous fuel diluted with nitrogen, and this decreases the energy efficiency in the product gas usage. The biomasses can also be gasified with steam, and this corresponds to steam gasification or steam reforming. In these processes, the product gas is not diluted at all. This can enhance the total efficiency. It has been found that $Rh/CeO_2/SiO_2$ was also effective in the steam gasification of biomass [14, 15]. However, the catalyst has problems in high cost and limited availability originated from the usage of Rh. Developments of metal catalysts for steam gasification of model compounds of biomass [16-19] and biomass itself [20] have also been carried out. Recently, we have investigated various oxides supported Ni catalysts in the steam gasification. As a result, it was found that CeO_2 support plays an important role on the decrease of coke deposition [21]. Furthermore, $Ni/CeO_2/Al_2O_3$ prepared by co-impregnation

method exhibited much higher performance than Ni/Al_2O_3 and $Ni/CeO_2/Al_2O_3$ prepared by sequential impregnation in the steam gasification of biomass [22, 23]. In this communication, we report the additive effect of Pt to $Ni/CeO_2/Al_2O_3$ prepared by co-impregnation method in the steam gasification of cedar wood, in particular, the effect of H_2 reduction pretreatment was also investigated.

Experimental

Catalyst

$Ni/CeO_2/Al_2O_3$ catalyst was prepared by co-impregnation method. An Al_2O_3 support (JRC-ALO-1) was impregnated with the aqueous solution of $Ni(NO_3)_2 \cdot 6H_2O$ (Wako Pure Chemical Industries) and $Ce(NH_4)_2(NO_3)_6$ (Wako Pure Chemical Industries) mixture by the incipient wetness method. Before the impregnation, Al_2O_3 was calcined in air at 1473 K to transform from γ-Al_2O_3 to α-Al_2O_3. The sample was dried at 383 K for 12 h followed by the calcination at 773 K for 3 h under air atmosphere. The $Ni/CeO_2/Al_2O_3$ catalyst modified with Pt was also prepared, and the modification method was as follows: calcined $Ni/CeO_2/Al_2O_3$ was impregnated with an aqueous solution of $Pt(NO_2)_2(NH_3)_2$ (Soekawa Chemical Co.,Ltd.). Subsequently, the sample was dried at 383 K for 12 h, and calcined again at 773 K in the air for 3 h. The catalyst obtained here is denoted as $Pt/Ni/CeO_2/Al_2O_3$. The Ni/Al_2O_3 catalyst was prepared as a reference by incipient wetness method using the Al_2O_3 and the aqueous solution of $Ni(NO_3)_2 \cdot 6H_2O$. After the loading of Ni, the catalyst was dried at 383 K for 12 h, and calcined at 773 K for 3 h under air atmosphere. All these catalysts were sieved to granules with the size of 0.16–0.35 mm. The loading amount of Ni was 4 wt%, and that of CeO_2 was 30 wt%. The loading amount of Pt was 0.1 wt%. As a reference, we also prepared

$Pt/CeO_2/Al_2O_3$ with the same loading amount as above, and the preparation method was also similar to that of $Pt/Ni/CeO_2/Al_2O_3$ except for the introduction of Ni.

Biomass

Cedar wood was ground with a ball mill to about 0.1–0.3 mm size. The moisture content of the cedar wood was 9.2%. The dry-based composition by weight was C 51.1 %, H 5.9 %, O 42.5 %, N 0.1 %, and ash 0.3 %. The elemental analysis was carried out by the Japan Institute of Energy.

Activity test of steam gasification of biomass

Steam gasification of biomass was carried out in a laboratory-scale continuous feeding dual-bed reactor. The reactor contained the primary bed for pyrolysis of biomass and accumulation of solid products in pyrolysis reaction such as char and ash. The products in the gas phase at reaction temperature can include tar and they were introduced to the secondary catalyst bed. The structure of the reactor has already been described in our previous reports, and the details of the procedure for catalytic performance evaluation in the steam gasification of cedar have been also shown [22, 23]. The biomass feeder consisted of a conical glass vessel with a screw valve at the bottom, allowing continuous feeding of biomass particles by vibrating the vessel with an electric vibrator. Nitrogen was used for transporting the biomass particles to the primary bed.

Feeding rate of gases, steam and biomass are described in each result. In the reaction, carbon-containing solid byproducts were observed. Here, the solid carbon deposited on the catalysts is called coke. The method to determine coke and char amount was the same as that in our previous report [22, 23]. The reaction temperature was controlled by the thermocouple

positioned outside the reactor. The tests were carried out under atmospheric pressure by using 1 g of catalyst. We evaluated the catalytic performance over the catalysts with or without H_2 reduction pretreatment. In order to remove any solid and liquid materials contained in the product gas, the effluent gas went through a filter and an iced water condenser and it was collected by a syringe and analyzed by a gas chromatograph (GC). The concentrations of CO, CO_2, CH_4 and C_2 (ethane and ethylene) were determined by FID-GC equipped with a methanator and that of H_2 was determined by TCD-GC. The flow rate of the gas was measured by a soap membrane meter. The carbon-based conversion to gas (C-conversion) was calculated by "A/B × 100", where A represents the formation rate of $CO + CO_2 + CH_4$ and B represents the total carbon supplying rate contained in the biomass. The yields of coke and char were calculated by (total amount of CO_2+CO in the combustion)/(total carbon amount in fed biomass). As a result, we can measure the yield of gaseous products and solid products (coke and char). On the other hand, it is difficult to determine the tar amount precisely. This is because tar is easily condensable in the reactor systems and a part of tar can not be collected. Therefore, we estimated the tar yield by subtraction of gaseous and solid products yields from the total. The yield of tar was defined as (100–C-conv. (%)–coke yield (%)–char yield (%)). In addition, we used the formation rate of $CO + H_2 + 4CH_4$ for the comparison, where 4 times of CH_4 is based on the reaction formula of $CH_4 + H_2O \rightarrow CO + 3H_2$. This is because the yield of the flammable gas is related to the energy efficiency in the utilization of biomass for power generation as well as the chemical utilization of produced synthesis gas. In our experiments, catalysts were used repeatedly. After the procedure of coke combustion, the same catalyst was applied to another activity test at different reaction temperature.

Catalyst characterization

Chemisorption of H_2 was carried out in a high-vacuum system by a volumetric method. Before H_2 adsorption measurement, the catalysts were treated in H_2 at 773 K for 0.5 h. H_2 adsorption was performed at room temperature. Gas pressure at adsorption equilibrium was about 1.1 kPa. The sample weight was about 0.2 g. The dead volume of the apparatus was about 60 cm^3. Dispersion was calculated on the basis of the total H_2 adsorption.

Temperature-programmed reduction (TPR) with H_2 was performed in fixed-bed flow reactor. The TPR profile of each sample was recorded from room temperature to 973 K under a flow of 5.0% H_2/Ar. The flow rate of 5.0% H_2/Ar was 30 ml/min, and the catalyst weight was 50 mg. The heating rate was 10 K/min and the temperature was maintained at 973 K for 30 min after it reached 973 K. The consumption of H_2 was monitored continuously with a TCD gas chromatograph equipped with frozen acetone trap in order to remove H_2O from the effluent gas.

The Pt L_3-edge EXAFS was measured at the BL-9C station of the Photon Factory at the High Energy Accelerator Research Organization in Tsukuba, Japan (Proposal No. 2004G280). The storage ring was operated at 2.5 GeV with a ring current of 300 - 450 mA. A Si(111) single crystal was used to obtain monochromatic X-ray beam. The monochromator was detuned to 60% of the maximum intensity to avoid higher harmonics in the X-ray beam. Two ion chambers filled with N_2 and 15% Ar diluted with N_2 were used to detect I_0 and I, respectively. The samples for the EXAFS measurement were prepared by pressing catalyst powder of 200 mg, and the thickness of the samples was chosen to be 1.5 mm (10 mmϕ) to give edge jump of 0.05. The sample was reduced with H_2 at 773 K for 0.5 h. After the pretreatment, the samples were transferred to the measurement cell without exposing the sample disk to air using a glove box filled with nitrogen. EXAFS data were

collected in a transmission mode at room temperature. For EXAFS analysis, the oscillation was first extracted from the EXAFS data by a spline smoothing method [24]. The oscillation was normalized by the edge height around 50 eV. The Fourier transformation of the k^3-weighted EXAFS oscillation from *k* space to *r* space was performed to obtain a radial distribution function. The inversely Fourier filtered data were analyzed by a usual curve fitting method [25, 26]. For the curve fitting analysis, the empirical phase shift and amplitude functions for the Pt-Pt bond were extracted from the data for Pt foil. Theoretical functions for the Pt-Ni bond were calculated using the FEFE8.2 program [27]. The analyses of EXAFS data were performed using the "REX2000" program (RIGAKU Co. Version: 2.3.3).

Results and discussion

Figure 1 shows catalytic performance in the steam gasification of biomass over Ni/Al_2O_3, $Ni/CeO_2/Al_2O_3$, $Pt/Ni/CeO_2/Al_2O_3$ with H_2 reduction. We carried out the activity test for 15 min. The formation of H_2, CO, CO_2 and CH_4 was observed, and their formation rates were almost stable during 15 min, although the coke deposition was observed as shown in figure 1. Generally speaking, coke deposition is one of the common and serious problems in the syngas production process [28-30]. Since the amount of coke represented by the weight ratio to the catalyst can be estimated to be at most 4 wt%, it is interpreted that the coke amount did not reach the level to cause the catalyst deactivation in the present case. Therefore, the average formation rates of these products for 15 min was applied, and they were represented in the results. On all these three catalysts, the yield of gas increased, in contrast, the yield of coke and char decreased with increasing reaction temperature. The difference in the catalyst performance among the catalysts is larger at lower reaction temperature. For example, the tar

yield on $Pt/Ni/CeO_2/Al_2O_3$ at 823 K was almost zero, and this indicates high activity of the steam reforming of tar. The order of the activity was as follows: $Pt/Ni/CeO_2/Al_2O_3$ > $Ni/CeO_2/Al_2O_3$ > Ni/Al_2O_3. The promoting effect of CeO_2 on Ni/Al_2O_3 can be caused by the strong interaction between Ni and CeO_2, which is effectively formed by the co-impregnation preparation method [22, 23]. One possible explanation of the role of this interaction is that CeO_2 can supply oxygen atom to the adsorbed species on Ni metal surface. It is expected that the carbonaceous reaction intermediate species adsorbed on Ni metal surface can react with oxygen atom supplied from neighboring CeO_2 [22, 23], where steam can compensate oxygen atom on CeO_2. Another and more important point is that $Pt/Ni/CeO_2/Al_2O_3$ has higher activity than $Ni/CeO_2/Al_2O_3$ and $Pt/CeO_2/Al_2O_3$. $Pt/CeO_2/Al_2O_3$ showed much lower performance in the steam gasification of biomass than $Ni/CeO_2/Al_2O_3$ because of much lower Pt loading than Ni. The synergetic effect between Pt and $Ni/CeO_2/Al_2O_3$ was clearly observed.

The amount of H_2 adsorption is listed in Table 1. Compared to $Ni/CeO_2/Al_2O_3$, $Pt/Ni/CeO_2/Al_2O_3$ showed larger amount of H_2 adsorption, and this can be related to high performance of $Pt/Ni/CeO_2/Al_2O_3$. In addition, $Ni/CeO_2/Al_2O_3$ had higher performance than Ni/Al_2O_3, on which H_2 adsorption amount was larger than that on $Ni/CeO_2/Al_2O_3$ due to the covering Ni with CeO_2 over $Ni/CeO_2/Al_2O_3$. This can be related to high performance caused by the interaction between Ni and CeO_2.

Figure 2 shows catalytic performance in the steam gasification of biomass over the catalysts without H_2 reduction. It is clearly seen that Ni/Al_2O_3 without reduction pretreatment showed much lower activity than that with reduction, and this means that H_2 reduction is necessary for the activation of Ni/Al_2O_3 and it is impossible to activate Ni/Al_2O_3 by the compounds contained in tar even at 923 K. In contrast, in the case of $Ni/CeO_2/Al_2O_3$,

the difference between the catalyst with and without H_2 reduction became much smaller, however, at 823 K, the yield of coke and tar on the catalyst can be decreased by the H_2 reduction pretreatment. On the other hand, $Pt/Ni/CeO_2/Al_2O_3$ showed very high activity even without H_2 reduction, and this indicates that H_2 reduction is not required for the activation of $Pt/Ni/CeO_2/Al_2O_3$. And this also means that $Pt/Ni/CeO_2/Al_2O_3$ can be activated by the compounds contained in the tar. It is suggested that the activation by tar compounds can be related to the catalyst reducibility. Therefore, catalysts were characterized by TPR. Figure 3 shows the TPR profiles of the calcined catalysts. On Ni/Al_2O_3, the H_2 consumption was observed in the temperature range between 630 K and 840 K. This can be assigned to the reduction of NiO interacted with α-Al_2O_3 surface [31]. On $Ni/CeO_2/Al_2O_3$, the H_2 consumption peak was shifted to lower temperature, and this can be due to the reduction of NiO interacted with CeO_2 on the basis of the reported results [21-23]. This is also supported by the results that the Ni-based reduction degree exceeded 100%, which corresponds to the reduction of CeO_2 together with Ni. In the case of $Pt/Ni/CeO_2/Al_2O_3$, a sharp H_2 consumption peak appeared at about 523 K. For the assignment of this reduction peak on $Pt/Ni/CeO_2/Al_2O_3$, the TPR profile of $Pt/CeO_2/Al_2O_3$ was also obtained. Only a small amount of H_2 consumption was observed on $Pt/CeO_2/Al_2O_3$. From the comparison between $Pt/CeO_2/Al_2O_3$ and $Pt/Ni/CeO_2/Al_2O_3$, the sharp peak at 523 K can be assigned to the reduction of NiO promoted by the presence of Pt, and strong interaction between Pt and Ni is expected like the alloy formation as mentioned below. This sharp peak corresponds to the reduction of about 25% Ni. In addition, a broad peak of $Pt/Ni/CeO_2/Al_2O_3$ was shifted to a little higher temperature than that of $Ni/CeO_2/Al_2O_3$. This phenomenon is due to the loss of 25% Ni reduction from the broad peak by the promoting effect of Pt. In fact, the Ni-based reduction degree exceeded 100%, which corresponds to the reduction of CeO_2 together with

Ni like $Ni/CeO_2/Al_2O_3$ and the temperature was clearly higher than Ni/Al_2O_3. The Ni species with high Pt-promoting reducibility can play important role on the activation of $Pt/Ni/CeO_2/Al_2O_3$ by tar compounds as a reductant at lower temperature. This result can contribute to the facilitation of the catalyst regeneration in the steam gasification of biomass, where catalysts can be deactivated by the deposited coke in a practical case. In this case, the catalysts should be regenerated by the combustion of coke, and the catalysts can be fully oxidized after this coke removal procedure. If the catalysts can be activated again without H_2 pretreatment, the practical operation will become easier. In fact, catalysts were used repeatedly in our experiments. This means that the same catalyst was applied to another activity test at different reaction temperature after the procedure of coke combustion. In this case, the coke combustion corresponds to the procedure for the catalyst regeneration in the practical case, and in this sense, the results contain the catalytic performance of regenerated catalysts.

Figure 4 shows the results of Pt L_3-edge EXAFS of $Pt/Ni/CeO_2/Al_2O_3$ after H_2 reduction at 773 K. In the FT spectra in Figure 4 (b), the peak of $Pt/Ni/CeO_2/Al_2O_3$ was observed at shorter distance than the Pt-Pt bond in Pt foil. The EXAFS spectrum of the $Pt/Ni/CeO_2/Al_2O_3$ can be fitted by the single Pt-Ni bond, and the coordination number and the bond distance was determined to be 7.3 and 0.252 nm, respectively. The bond distance is close to that of the Ni-Ni bond (0.249 nm) in Ni metal, and this suggests the formation of Pt-Ni alloy phase where the Pt atoms can partly substitute Ni atoms in Ni metal phase. These structural properties are supported by the previous report on the alloy formation of Pt-Ni [32]. Furthermore, it has been reported that the Pt-Ni alloy formation enhanced the catalytic activity in methane reforming [33], and this report can support the present result.

Figure 5 shows the results of Ni *K*-edge EXAFS analysis of three Ni catalysts (Ni/Al_2O_3, $Ni/CeO_2/Al_2O_3$, $Pt/Ni/CeO_2/Al_2O_3$) after the H_2 reduction at 773 K. The curve fitting results are listed in Table 2. All the peaks at around 0.21 nm shown in Fig. 5 (b) can be assigned to the Ni-Ni bond, and it is found that the CN of Ni-Ni bond on $Pt/Ni/CeO_2/Al_2O_3$ was almost the same as that on $Ni/CeO_2/Al_2O_3$ and smaller than that on Ni/Al_2O_3. As shown in Table 2, $Pt/Ni/CeO_2/Al_2O_3$ can be fitted without the Ni-Pt bond in the Ni *K*-edge EXAFS analysis, although it can be fitted by only Pt-Ni bond in the Pt L_3-edge EXAFS analysis. This can be explained by the very low molar ratio of Pt/Ni=1/75. It is concluded that the metal particle size of Ni on $Pt/Ni/CeO_2/Al_2O_3$ can be almost the same as that on $Ni/CeO_2/Al_2O_3$, and the average particle size of Ni can be estimated to be 7.0 ± 0.9 nm [22, 34]. Therefore, in the promoting effect of Pt, the change of metal size can be excluded. The promoting effect of Pt is to enhance the catalytic activity by the Pt-Ni alloy formation and the catalyst reducibility by the property of Pt itself.

Conclusions

Additive effect of Pt to $Ni/CeO_2/Al_2O_3$ catalysts prepared by the co-impregnation method was investigated in the steam gasification of biomass comparing to $Ni/CeO_2/Al_2O_3$ and Ni/Al_2O_3. On these three catalysts with H_2 reduction pretreatment, the performance was $Pt/Ni/CeO_2/Al_2O_3$ > $Ni/CeO_2/Al_2O_3$ > Ni/Al_2O_3. The EXAFS analysis indicates the Pt-Ni alloy formation on the $Pt/Ni/CeO_2/Al_2O_3$, and this can be related to high performance in the steam gasification of biomass. Furthermore, $Ni/CeO_2/Al_2O_3$ and Ni/Al_2O_3 showed lower performance without H_2 reduction. In contrast, the performance of $Pt/Ni/CeO_2/Al_2O_3$ without H_2 reduction was as high as that with H_2 reduction, and this means that the catalyst can be activated easily with the compounds contained in the tar. According to the profiles of

the temperature programmed reduction with H_2, the addition of Pt promotes the reduction of Ni, and this can be related to the addition of Pt makes the reduction pretreatment unnecessary.

References

[1] A. V. Bridgwater, Appl. Catal. A: Gen. 116 (1994) 5.

[2] L. Devi, K. J. Ptasinski, F. J. J. G. Janssen, Biomass Bioenergy 24 (2003) 125.

[3] D. Sutton, B. Kelleher, J.R.H. Ross, Fuel Proc. Technol. 73 (2001) 155.

[4] K. Tomishige, M. Asadullah, K. Kunimori, Catal. Today 89 (2004) 389.

[5] M. Asadullah, K. Tomishige, K. Fujimoto, Catal. Commun. 2 (2001) 63.

[6] M. Asadullah, S. Ito, K. Kunimori, M. Yamada, K. Tomishige, J. Catal. 208 (2002) 255.

[7] M. Asadullah, S. Ito, K. Kunimori, M. Yamada, K. Tomishige, Environ. Sci. Technol. 36 (2002) 4476.

[8] M. Asadullah, T. Miyazawa, S. Ito, K. Kunimori, K. Tomishige, Appl. Catal. A: Gen. 246 (2003) 103.

[9] M. Asadullah, T. Miyazawa, S. Ito, K. Kunimori, M. Yamada, K. Tomishige, Appl. Catal. A: Gen. 255 (2003) 169.

[10] M. Asadullah, T. Miyazawa, S. Ito, K. Kunimori, S. Koyama, K. Tomishige, Biomass Bioenergy 26 (2004) 269.

[11] M. Asadullah, T. Miyazawa, S. Ito, K. Kunimori, M. Yamada, K. Tomishige, Appl. Catal. A: Gen. 267 (2004) 95.

[12] K. Tomishige, T. Miyazawa, T. Kimura, K. Kunimori, Catal. Commun. 6 (2005) 37.

[13] K. Tomishige, T. Miyazawa, T. Kimura, K. Kunimori, N. Koizumi, M. Yamada, Appl. Catal. B: Environ. 60 (2005) 299.

[14] M. Asadullah, T. Miyazawa, S. Ito, K. Kunimori, K. Tomishige, Energy Fuels 17 (2003) 842.

[15] K. Tomishige, T. Miyazawa, M. Asadullah, S. Ito, K. Kunimori, J. Jpn. Petrol. Inst. 46 (2003) 322.

[16] D. Wang, D. Montane, E. Chornet, Appl. Catal. A: Gen. 143 (1996) 245.

[17] D.N. Bangala, N. Abatzoglou, E. Chornet, AICHE J. 44 (1998) 927.

[18] T. Furusawa, A. Tsutsumi, Appl. Catal. A: Gen. 278 (2005) 207.

[19] T. Furusawa, A. Tsutsumi, Appl. Catal. A:Gen. 278 (2005) 195.

[20] L. Garcia, A. Benedicto, E. Romeo, M. L. Salvador, J. Arauzo, R. Bilbao, Energy Fuels 16 (2002) 1222.

[21] T. Miyazawa, T. Kimura, J. Nishikawa, S. Kado, K. Kunimori, K. Tomishige, Catal. Today 115 (2006) 254.

[22] T. Kimura, T. Miyazawa, J. Nishikawa, T. Miyao, S. Naito, K. Okumura, K. Kunimori, K. Tomishige, Appl. Catal. B: Envrion., 68 (2006) 160.

[23] K. Tomishige, T. Kimura, J. Nishikawa, T. Miyazawa, K. Kunimori, Catal. Commun. 8 (2007) 1074.

[24] J.W. Cook, D.E. Sayers, J. Appl. Phys. 52 (1981) 5024.

[25] K. Okumura, J. Amano, N. Yasunobu, M. Niwa, J. Phys. Chem. B 104 (2000) 1050.

[26] K. Okumura, S. Matsumoto, N. Nishiaki, M. Niwa, Appl. Catal. B: Environ. 40 (2003) 151.

[27] A.L. Ankudinov, B. Ravel, J.J. Rehr, S.D. Conradson, Phys. Rev. B 58 (1998) 7565.

[28] K. Tomishige, Y. Himeno, Y. Matsuo, Y. Yoshinaga, Y. Fujimoto, Ind. Eng. Chem. Res. 39 (2000) 1891.

[29] K. Tomishige, Y.G. Chen, K. Fujimoto, J. Catal. 181 (1999) 91.

[30] C.H. Bartholomew, Catal. Rev. Sci. Eng. 24 (1982) 67.

[31] B.T. Li, R. Watanabe, K. Maruyama, M. Nurunnabi, K. Kunimori, K. Tomishige, Appl. Catal. A:Gen. 290 (2005) 36.

[32] B.T. Li, S. Kado, Y. Mukainakano, T. Miyazawa, T. Miyao, S. Naito, K. Okumura, K. Kunimori, K.Tomishige, J. Catal., 245 (2007) 144.

[33] Y.G. Chen, K. Tomishige, K. Yokoyama, K. Fujimoto, Appl. Catal. A:Gen. 165 (1997) 335

[34] R.B.Greegor, F.W.Lytle, J. Catal. 63 (1980) 476.

Table 1. Results of TPR and H_2 adsorption on various catalysts.

Catalysts	Loading amount / 10^{-3} mol g^{-1}-cat		H_2 adsorption H/Ni[a)]	H_2 consumption[b)] / 10^{-3} mol g^{-1}-cat	Ni-based reduction degree[c)] / %	Reduction degree of CeO_2[d)]/ %	BET Surface Area/ m^2 g^{-1}
	Ni	Pt					
Ni/Al_2O_3	0.68	0	0.066	0.71	104	-	9
$Ni/CeO_2/Al_2O_3$	0.68	0	0.058	1.01	156	46	13
$Pt/Ni/CeO_2/Al_2O_3$	0.68	0.005	0.084	0.97	142	34	15

a) Total hydrogen adsorption at 298 K.
b) H_2 consumption in TPR profiles shown in Figure 3.
c) Assuming that $Ni^{2+}+H_2 \rightarrow Ni^0+2H^+$
d) H_2 consumption over 100% Ni-based reduction degree was assigned to the reduction of CeO_2, assuming that $2CeO_2+H_2 \rightarrow Ce_2O_3+H_2O$.

Table 2 Curve fitting results of Ni-*K* edge EXAFS of various Ni catalysts after reduced at 773 K.

Catalyst	Shells	CN^a	R / 10^{-1} nm^b	σ / 10^{-1} nm^c	ΔE_0 / eV^d	R_f / %^{e}
Ni/Al_2O_3	Ni-Ni	11.3±0.2	2.49±0.001	0.065±0.002	1.0±0.3	0.3
$Ni/CeO_2/Al_2O_3$	Ni-Ni	9.4±0.3	2.48±0.002	0.077±0.003	-0.8±0.4	0.4
$Pt/Ni/CeO_2/Al_2O_3$	Ni-Ni	9.3±0.2	2.49±0.002	0.078±0.003	-0.7±0.4	1.0
Ni Foil	Ni-Ni	12.0	2.49	0.06	0	

[a]Coordination number. [b]Bond distance. [c]Debye-Waller factor. [d]Difference in the origin of photoelectron energy between the reference and the sample. [e]Residual factor.

Fourier transform range: 30-142 nm^{-1}, Fourier filtering range: 0.138-0.295 nm.

Figure captions

Figure 1. Catalytic performance in steam gasification of biomass over the catalysts with H_2 reduction.

Conditions: biomass; 60 mg/min (H_2O 9.2 %, C 2191 μmol/min; H 3543 μmol/min; O 1475 μmol/min), N_2 flow rate; 60 cc/min, (added H_2O)/C=0.5 (steam flow rate 1110 μmol/min), reaction time; 15 min, H_2 reduction 773 K, 30 min.

Figure 2. Catalytic performance in steam gasification of biomass over the catalysts without H_2 reduction.

Conditions: biomass; 60 mg/min (H_2O 9.2 %, C 2191 μmol/min; H 3543 μmol/min; O 1475 μmol/min), N_2 flow rate; 60 cc/min, (added H_2O)/C=0.5 (steam flow rate 1110 μmol/min), reaction time; 15 min.

Figure 3. TPR profiles of the catalysts.

TPR conditions: heating rate 10 K/min, Room temperature to 973 K, and the temperature was maintained at 973 K for 30 min. Flow rate of 5% H_2/Ar : 30 ml/min

Sample weight : 50 mg-cat.

Figure 4. Results of Pt L_3-edge EXAFS analysis of the catalysts reduced at 773 K.

(a) k^3-weighted EXAFS oscillations, Fourier filtered EXAFS data (solid line), and calculated data (dotted line). Fourier filtering range : 0.160-0.267 nm.

(b) Fourier transforms of k^3-weighted Pt L_3-edge EXAFS, FT range : 30-128 nm^{-1}.

Figure 5. Results of Ni *K*-edge EXAFS analysis of reduced catalysts.

(a)k^3-weighted EXAFS oscillations.

(b) Fourier transform of k^3-weighted Ni *K*-edge EXAFS. FT range : 30-142 nm^{-1}.

(c) Fourier filtered EXAFS data (solid line) and calculated data (dotted line). Fourier filtering range : 0.138-0.295 nm.

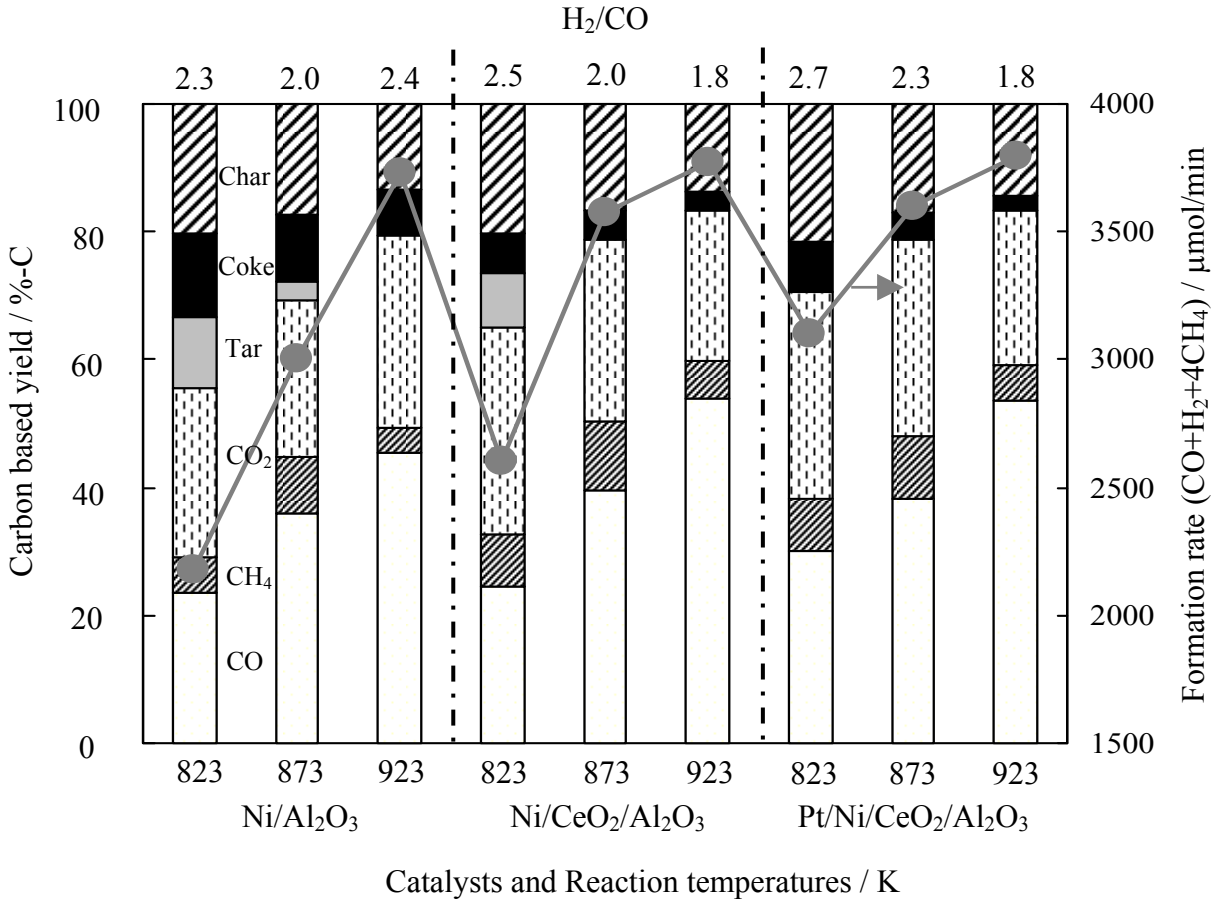

Figure 1. Catalytic performance in steam gasification of biomass over the catalysts with H_2 reduction.
Conditions: biomass; 60 mg/min (H_2O 9.2 %, C 2191 μmol/min; H 3543 μmol/min; O 1475 μmol/min), N_2 flow rate; 60 cc/min , (added H_2O)/C=0.5 (steam flow rate 1110 μmol/min), reaction time; 15 min. H_2 reduction 773 K, 30 min.

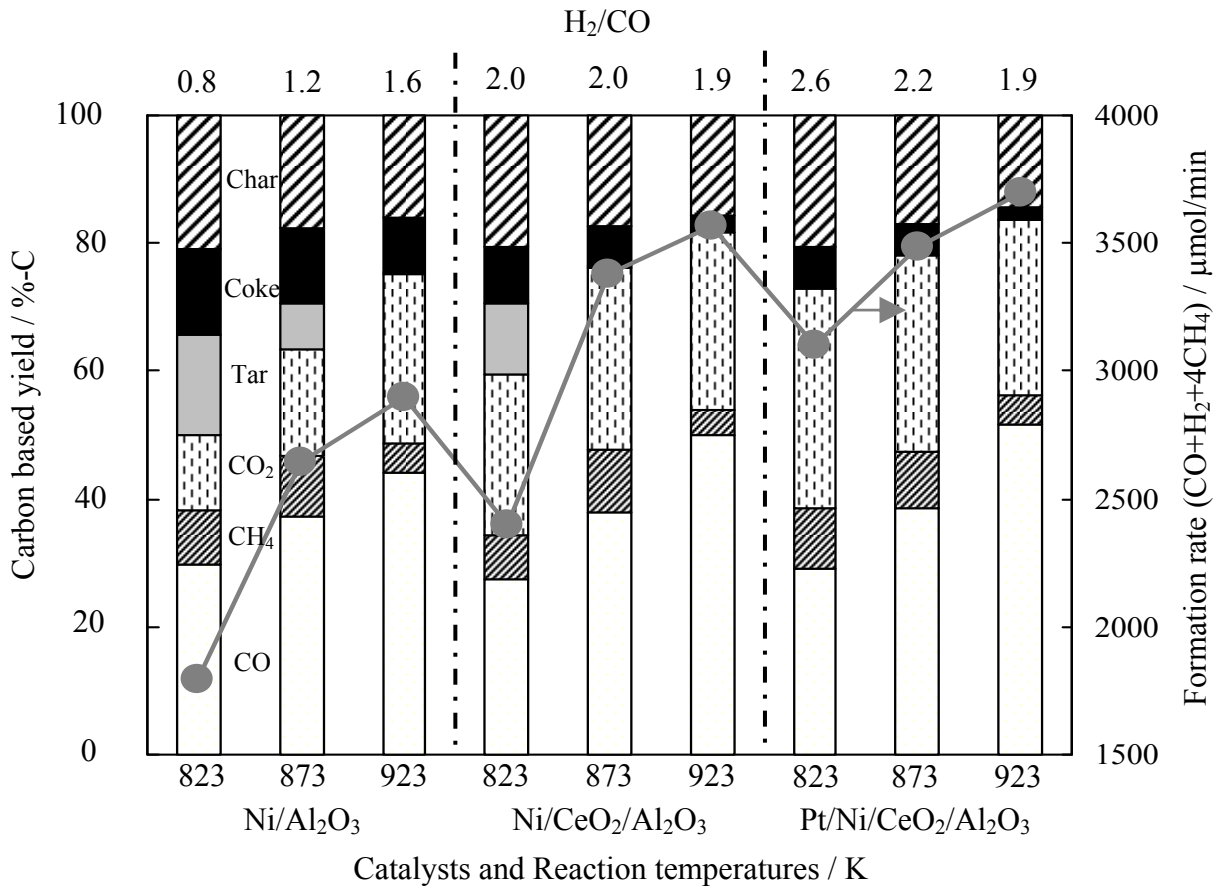

Figure 2. Catalytic performance in steam gasification of biomass over the catalysts without H_2 reduction.
Conditions: biomass; 60 mg/min (H_2O 9.2 %, C 2191 μmol/min; H 3543 μmol/min; O 1475 μmol/min), N_2 flow rate; 60 cc/min, (added H_2O)/C=0.5 (steam flow rate 1110 μmol/min), reaction time; 15 min.

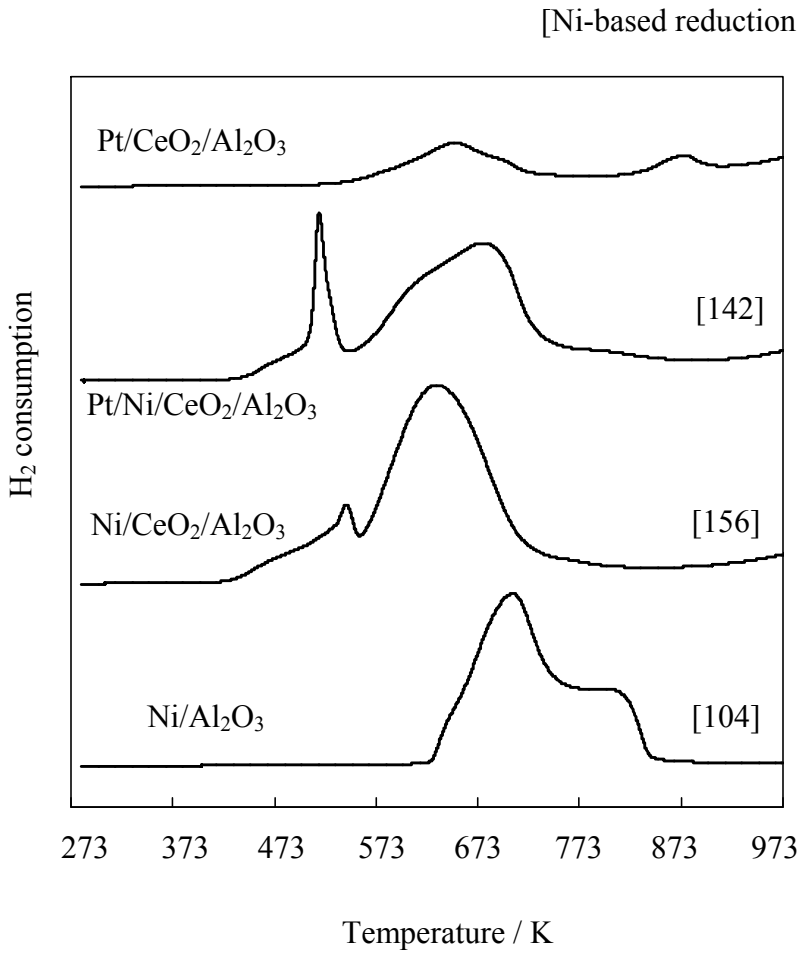

Figure 3. TPR profiles of the catalysts.
TPR conditions: heating rate 10 K/min, Room temperature to 973 K, and the temperature was maintained at 973 K for 30 min. Flow rate of 5% H_2/Ar : 30 ml/min
Sample weight : 50 mg-cat.
Ni-based reduction degree was based on the assumption of $Ni^{2+} + H_2 \rightarrow Ni^0 + 2H^+$, and the contribution of Pt was neglected.

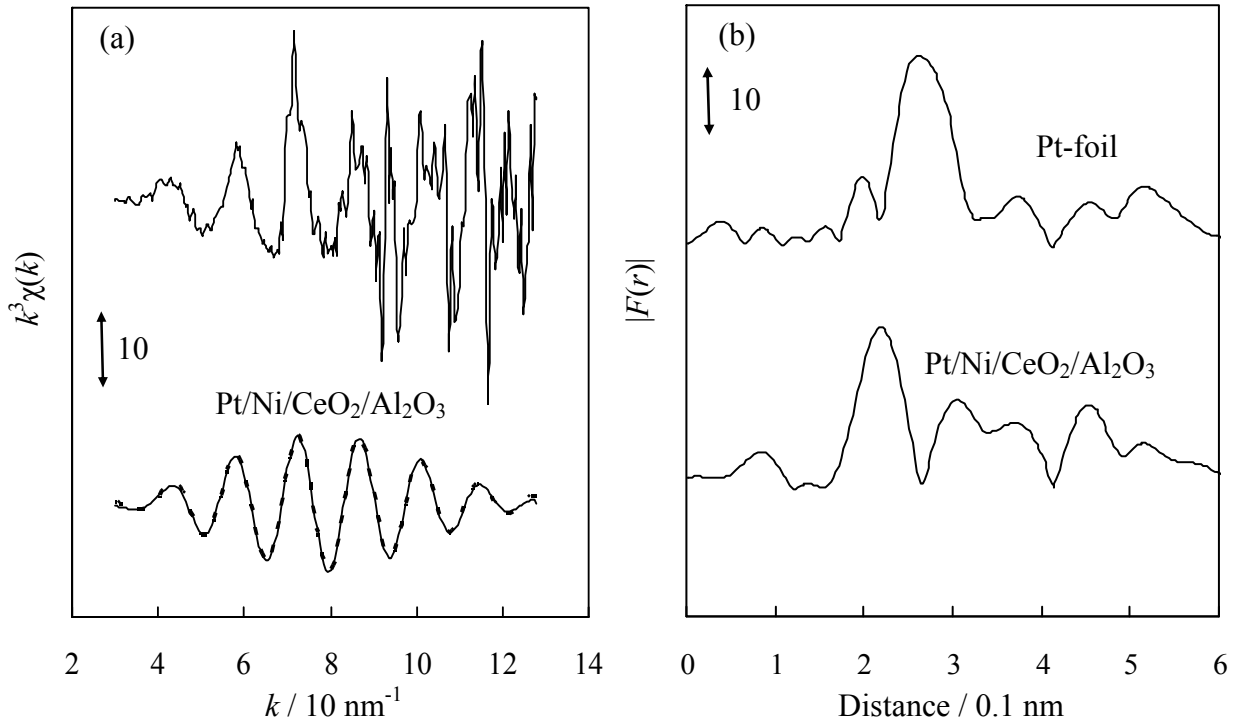

Figure 4. Results of Pt L_3-edge EXAFS analysis of the catalysts reduced at 773 K.
(a) k^3-weighted EXAFS oscillations, Fourier filtered EXAFS data (solid line), and calculated data (dotted line). Fourier filtering range : 0.160-0.267 nm.
(b) Fourier transforms of k^3-weighted Pt L_3-edge EXAFS, FT range : 30-128 nm^{-1}.

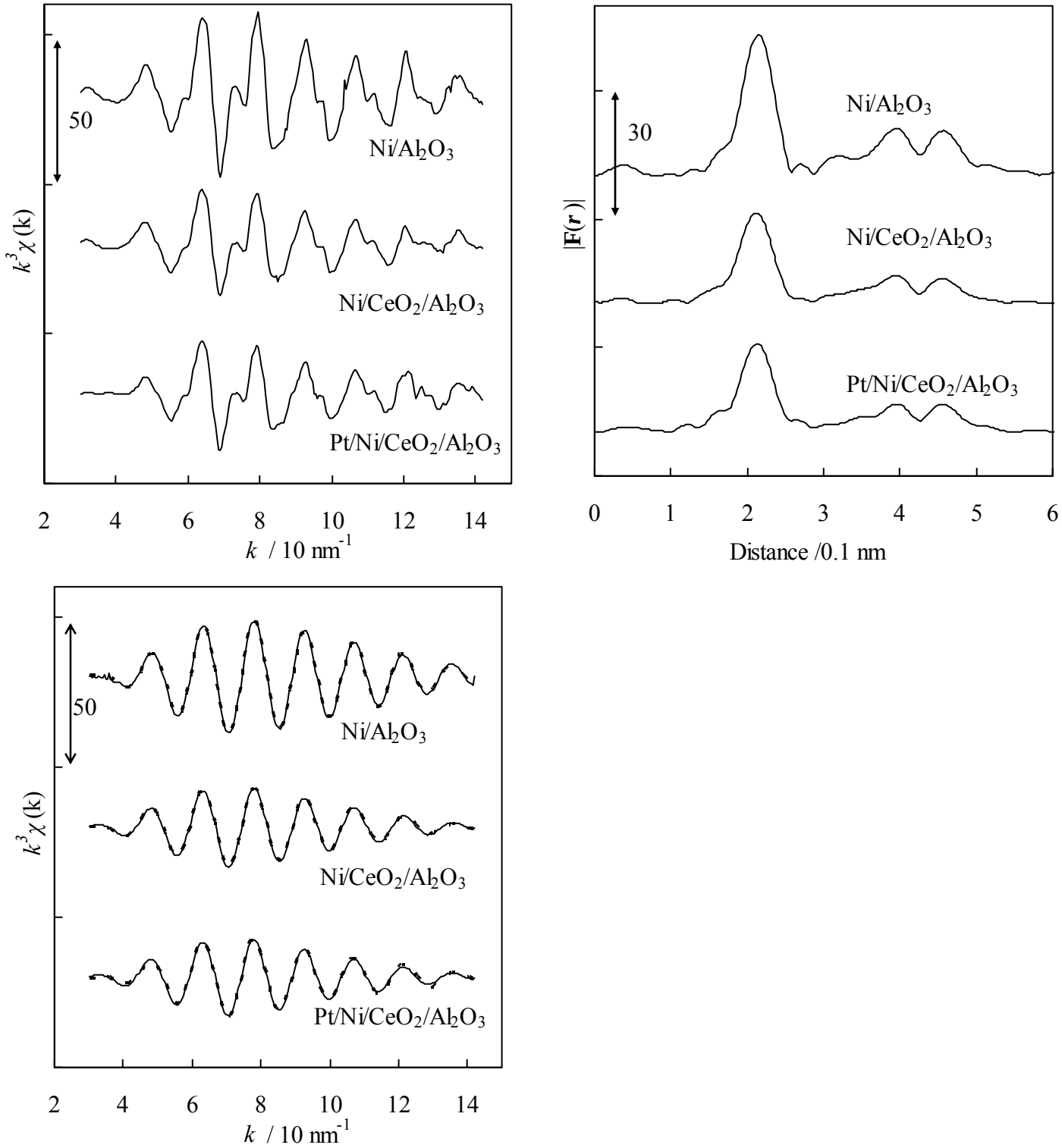

Figure 5. Results of Ni *K*-edge EXAFS analysis of reduced catalysts.

(a)k^3-weighted EXAFS oscillations.

(b) Fourier transform of k^3-weighted Ni *K*-edge EXAFS

FT range : 30-142 nm^{-1}.

(c) Fourier filtered EXAFS data (solid line) and calculated data (dotted line)

Fourier filtering range : 0.138-0.295 nm.